Free Oscillations in a Climate Model with Ice-Sheet Dynamics

E. KÄLLÉN[1] AND C. CRAFOORD

Department of Meteorology, Arrhenius Laboratory, Stockholm University, S-10691 Stockholm, Sweden

M. GHIL

Courant Institute of Mathematical Sciences, New York University, New York 10012

(Manuscript received 3 April 1979, in revised form 17 July 1979)

ABSTRACT

A study of stable periodic solutions to a simple nonlinear model of the ocean-atmosphere-ice system is presented. The model has two dependent variables: ocean-atmosphere temperature and latitudinal extent of the ice cover. No explicit dependence on latitude is considered in the model. Hence all variables depend only on time and the model consists of a coupled set of nonlinear ordinary differential equations.

The globally averaged ocean-atmosphere temperature in the model is governed by the radiation balance (Budyko, 1969; Sellers, 1969). The reflectivity to incoming solar radiation, i.e., the planetary albedo, includes separate contributions from sea ice and from continental ice sheets. The major physical mechanisms active in the model are 1) albedo-temperature feedback, 2) continental ice-sheet dynamics (Weertman, 1964, 1976) and 3) precipitation-rate variations.

The model has three equilibrium solutions, two of which are linearly unstable, while one is linearly stable. For some choices of parameters, the stability picture changes and sustained, finite-amplitude oscillations obtain around the previously stable equilibrium solution. The physical interpretation of these oscillations points to the possibility of internal mechanisms playing a role in glaciation cycles.

1. Introduction

In trying to understand climatic variability, one of the first questions to ask is: has the climate changed due to *external* or *internal* causes? By external causes we mean agencies outside the atmosphere - hydrosphere - cryosphere - biosphere - lithosphere system. An example of such external agencies are astronomically caused changes in the earth's orbital parameters. The astronomical theory of climatic change, also called the Milankovitch theory, appears to be successful in explaining some of the climatic variability on time scales between 10^4 and 10^5 years (Mitchell, 1976; Hays *et al.*, 1976); an important fraction of this variability, however, remains unexplained at this point by such external causes (Kominz and Pisias, 1979).

Internal causes, on the other hand, are processes or mechanisms present within the atmosphere-hydrosphere - cryosphere - biosphere - lithosphere system, giving rise to self-excited climate fluctuations. The purpose of this article is to investigate, in its simplest form, the possible contribution of such internal causes to climatic variability on long time scales. Under certain simplifying assumptions, internal mechanisms can be modeled by a set of ordinary differential equations (ODE's), and the general properties of the solution to such a system can be analyzed along the lines suggested by Lorenz (1963).

In nature, of course, the physical, chemical and biological processes are so numerous and so complex that it is impossible to set up a system of ODE's giving an adequate description of all the mechanisms involved. To gain some understanding of the climate system, one may try to isolate just a few components of this system, while some others are taken into account parametrically; still others might be considered less important and disregarded altogether.

In particular, various mechanisms act on different time scales; one could concentrate on modeling just one part of the climate spectrum and isolate those mechanisms involved in that part of the spectrum. The assumption is then that all processes faster than the ones studied are parameterized, while the slower processes are kept constant.

In the present study we use an energy-balance model of the atmosphere-hydrosphere system. Our intention is to study time-scales of the order of 10^3–10^5 years; hence the model takes the dynamics of continental ice sheets explicitly into account. The model is described in Section 2. The details of the simplified ice-sheet dynamics used in the model

[1] Present affiliation: European Center for Medium Range Weather Forecasts, Reading, Berkshire RG2 9AX, England.

0022-4928/79/122292-12$07.00

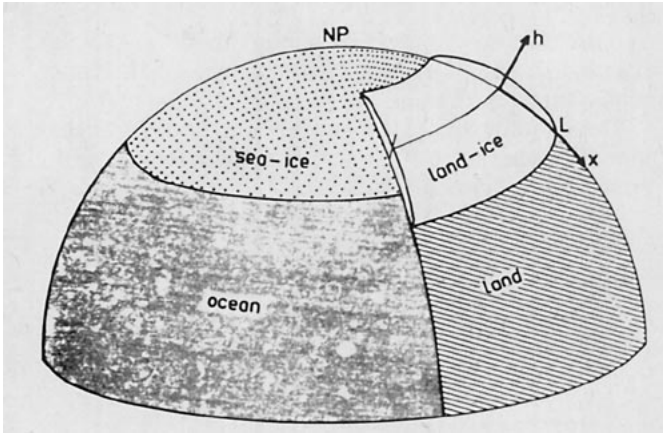

FIG. 1. A hemispherical picture of the model formulation.

appear in Section 3. The time-dependent behavior of the model is discussed in Section 4. Concluding remarks follow in Section 5.

A preliminary presentation of this work appears in Källén *et al.* (1978). The main difference between this article and the preceding one lies in the parameterization of the 0°C isotherm: previously it was taken as a vertical line with respect to the earth's surface, while here it is taken more realistically as a slanting line.

2. Model description

Our energy-balance equation is similar to the one originally proposed by Budyko (1969) and by Sellers (1969). The equation describing the flow of continental ice sheets follows Weertman (1976), who based it on his earlier ice-sheet model (Weertman, 1964).

The equations governing the model are

$$c_T \frac{dT}{dt} = R_i(T,L) - R_o(T), \tag{1a}$$

$$c_L \frac{dL}{dt} = F(T,L), \quad L \geq 0, \tag{1b}$$

where the two dependent variables are globally averaged temperature T and latitudinal extent of the land ice-cover L (Figs. 1 and 2). Here T is the mass average of ocean temperature and atmospheric temperature: the atmosphere is assumed to be in thermal equilibrium with the ocean on the time scale under investigation. For obvious physical reasons, L must be greater than zero.

R_i denotes the shortwave radiation absorbed by the system, R_o the longwave radiation emitted by the system, and F is a nonlinear function to be described in Section 3. The heat capacity c_T of the atmosphere-hydrosphere system governs its relaxation time, while c_L governs the relaxation time of the continental ice sheets. The ratio c_L/c_T will play an important role in our investigation.

The outgoing longwave radiation R_o has a linear dependence on temperature T (Budyko, 1969), given by

$$R_o(T) = k(T - T_0), \tag{2}$$

with T_0 and k constants. The dependence of absorbed incoming shortwave radiation R_i on the solar input Q and on the albedo α is given by

$$R_i(T,L) = Q\{1 - [\gamma\alpha_{\text{land}}(L) + (1 - \gamma)\alpha_{\text{ocean}}(T)]\}. \tag{3}$$

The planetary albedo is divided into two parts: α_{land} for continental areas and α_{ocean} for oceanic areas. The fraction of the earth covered by continents is denoted by γ.

The land albedo in the model depends on the extent of the land ice cover. We take α_{land} to be a linear function of L, i.e.,

$$\alpha_{\text{land}} = \alpha_0 + \alpha_1 L. \tag{4a}$$

Minimum and maximum values in α_{land} are reached when $L = 0$ (no land ice) and $L = L_{\max}$ (ice-covered continent), implying

$$\alpha_0 \leq \alpha_{\text{land}} \leq \alpha_0 + \alpha_1 L_{\max}. \tag{4b}$$

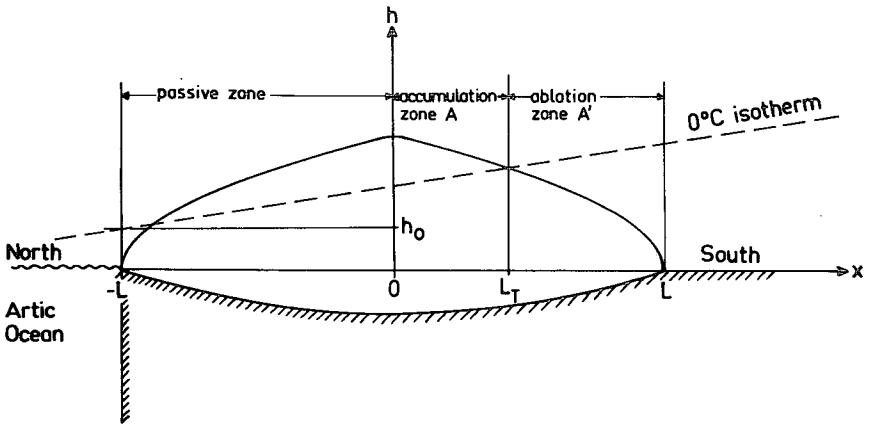

FIG. 2. Meridional cross section of the ice sheet.

This inequality will enable us to estimate α_0 and α_1 from the values of α tabulated by Sellers (1969), after having decided on a suitable scaling for L (see Section 3). Our land-ice model describes conditions resembling those of the Northern Hemisphere. We assume the Southern Hemisphere to be passively coupled to the Northern Hemisphere, on the time scale considered.

The quantity α_{ocean} is taken to be a function of the model temperature T in a way similar to that proposed by Sellers (1969) (cf. Fig. 3):

$$\alpha_{\text{ocean}} = \begin{cases} \alpha_{\text{max}}, & T \leq T_{\alpha,\text{lower}} \\ \dfrac{\alpha_{\text{min}} - \alpha_{\text{max}}}{T_{\alpha,\text{upper}} - T_{\alpha,\text{lower}}} (T - T_{\alpha,\text{lower}}) + \alpha_{\text{max}}, & T_{\alpha,\text{lower}} < T \leq T_{\alpha,\text{upper}} \\ \alpha_{\text{min}}, & T_{\alpha,\text{upper}} < T. \end{cases} \tag{5}$$

The formation and melting of sea ice occur much faster than the relaxation time scale of the atmosphere-hydrosphere system; in defining α_{ocean} it is assumed that they occur instantaneously. In Fig. 1 a qualitative picture of the model is given. Note that the dependent variables T and L are functions of time t only, i.e., no explicit latitude dependence appears in the model.

The aim of the present work is modeling some physical relations that give rise to self-induced oscillations, rather than attempting a detailed quantitative description of climatic oscillations. In order to obtain more reliable quantitative results, the latitudinal dependence of model variables would have to be taken into account.

3. Continental ice-sheet dynamics

In describing the dynamics of the continental ice sheets, we have used a model originally proposed by Weertman (1964). A modified version of the ice-sheet model is described by Weertman (1976) and our approach closely follows this later version. In connection with the growth and shrinkage of the land ice sheets, we have parameterized precipitation efficiency, taken by Weertman (1964, 1976) to be constant, as a function of temperature. In this way we try to take into account the temperature dependence of evaporation and atmospheric water content.

It is important to remember that all the considerations in this section lead to a simple relationship between the change in global ice-sheet volume, on the one hand, and global temperature and latitudinal ice-sheet extent on the other. The latitudinal distribution of the ice sheet and of the phenomena which contribute to changing its volume is only introduced conceptually, in order to formulate parametrically the desired global relationship.

a. Geometry of the ice sheet and the snowline

Consider then a circumpolar ring of ice, a part of which is seen in Fig. 1. If the ice flow is assumed to be zonally symmetric, we need only study a north-south cross section of the sheet (Fig. 2). Assuming that the ice sheet flows as a perfectly plastic substance, it will have a piecewise parabolic profile, symmetric about a vertical axis, given by

$$H(x) = \lambda^{1/2}(L - |x|)^{1/2}. \tag{6}$$

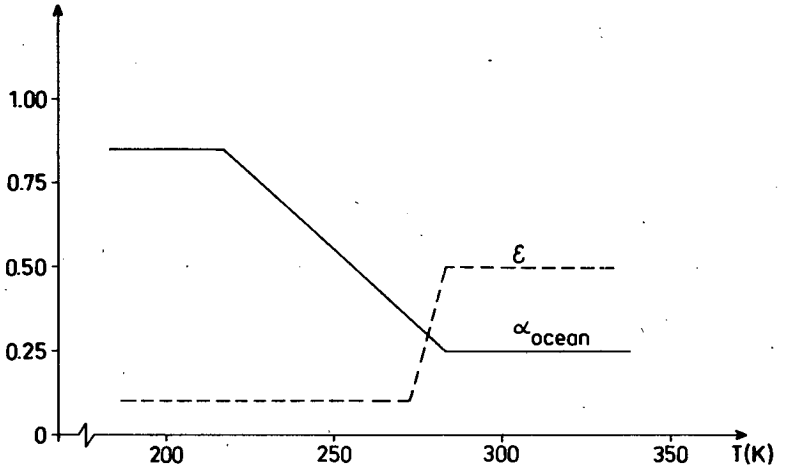

FIG. 3. Ocean albedo (α_{ocean}) and ratio of accumulation rate to ablation rate (ϵ) as functions of temperature (T).

Here H is the elevation of the ice at a distance x from the symmetry axis of the sheet, λ is a parameter with the dimensions of length given by $\lambda = (4/3) \times \tau/\rho g$, τ is the shear stress at the bottom of the sheet, taken to equal the yield stress, ρ is the ice density and g the acceleration of gravity. Also included in the ice model is the isostatic adjustment to the ice load of the continent below. This adjustment is assumed here to be instantaneous, making the total ice depth $\frac{3}{2}H$. For convenience, the height H is scaled with $\lambda^{1/2}$, yielding the new variable $h = H/\lambda^{1/2}$.

The x, h coordinate system is fixed relative to the symmetry axis of the ice sheet, while the northern edge of the ice sheet is fixed at the Arctic Ocean coastline (Fig. 2). Following Weertman (1976), we introduce a slanting 0°C isotherm, whose intersection with the surface of the ice sheet will give the dividing line between the ablation and accumulation areas, called the *snowline*. The 0°C isotherm, which depends implicitly on the global temperature T, is given in our model by

$$h(x) = h(x; T) = h_0(T) + s(x + L), \tag{7}$$

where h_0 is the height of the isotherm at the coastline of the Arctic Ocean, $x = -L$, and s is the slope of the isotherm, taken here to be constant, independent of T. Notice that because of the scaling of h, s has dimension of length to the $-\frac{1}{2}$ power.

The slope s of the 0°C isotherm could also be parameterized as a function of global temperature T. The effect of changes in s does not seem to be very important, at least qualitatively. In fact, the same results as here were obtained in Källén *et al.* (1978), where the isotherm was taken to be vertical.

We let the height $h_0(T) = h(-L; T)$ of the 0°C isotherm at $x = -L$ be governed by the atmosphere-ocean temperature T, i.e.,

$$h_0 = \beta(T - T_{00}). \tag{8}$$

Here T_{00} is the globally averaged temperature for which the 0°C isotherm would intersect the Arctic coastline. Thus T_{00} is close to, but conceivably somewhat lower than $T_{\alpha,\text{upper}}$; the difference between the two depends on whether the Arctic Ocean is ice covered or open [cf. assumption (i) below]. Such a functional relationship between h_0 and T is physically reasonably, but no direct reliable estimates of β seem to be readily available in the literature.

To determine the parameter β as a function of the other parameters in the problem, we make the following assumptions:

(i) The intersection between the 0°C isotherm and sea level follows the latitude of the southern edge of *sea* ice.

(ii) The land albedo is bounded by a maximum value, $\alpha_{\text{land,max}}$, obtained when L has its maximum value, $L_{\max}$.

Using (4b) we find from (ii) that

$$L_{\max} = \frac{\alpha_{\text{land,max}} - \alpha_0}{\alpha_1}. \tag{9a}$$

The physical model of the land ice sheet is no longer valid for $L > L_{\max}$, and the value of $L_{\max}$ has to be used as an upper bound on L. Using assumption (i) when $T = T_{\alpha,\text{lower}}$, i.e., when ocean ice has reached its maximum extent, substituting Eq. (8) into (7), and solving for β when $h(L) = 0$ and $L = L_{\max}$, we obtain

$$\beta = \frac{2sL_{\max}}{T_{00} - T_{\alpha,\text{lower}}} = \frac{2s(\alpha_{\text{land,max}} - \alpha_0)}{(T_{00} - T_{\alpha,\text{lower}})\alpha_1}. \tag{9b}$$

In modeling the dynamics of the ice sheet, one is interested in the mass balance of the sheet. Having fixed the northern edge of the sheet, we must assume that the dynamics of the whole sheet is governed by the mass balance of the southern half, following Weertman (1976). The northern half is then assumed to be in equilibrium with the southern half.

To calculate the mass balance of the southern half, we divide the ice into an ablation zone of area A', and an accumulation zone of area A (Fig. 2). These zones are separated by the snowline, the position of which is governed by the height of the 0°C isotherm. Because of the slanting isotherm, two snowlines may occur, but only the one on the southern half of the sheet is relevant to the mass balance. For positive slopes of the 0°C isotherm, $s > 0$, we can at most have one snowline on the southern half of the sheet. The position of this snowline, $x = L_T$, is given by equating the values of $h(x)$ from (6) and (7); the result is

$$h(L_T) = (L - L_T)^{1/2} = h_0 + s(L_T + L). \tag{10a}$$

Solving for L_T yields

$$L_T = s^{-2}[(2s^2L + sh_0 + \tfrac{1}{4})^{1/2} - (s^2L + sh_0 + \tfrac{1}{2})]. \tag{10b}$$

b. *Mass balance of the ice sheet*

The change of mass or, equivalently, the change of volume of the ice sheet is calculated by setting up a continuity equation for the ice sheet. It states that the rate of change of the volume V is given by the difference between the total accumulation and the total ablation rates:

$$\frac{dV}{dt} = aA - a'A', \tag{11}$$

where a and a' are the accumulation and ablation rates per unit area, respectively; a and a' have the

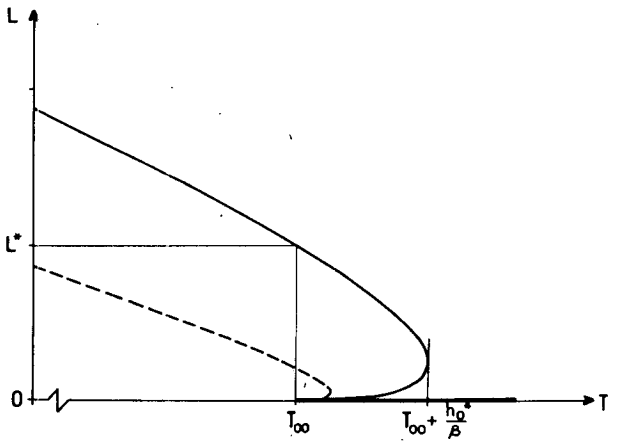

FIG. 4. Equilibrium ice-sheet size L plotted against temperature T for two different values of ϵ. Solid curve gives the equilibrium for $\epsilon = \epsilon_{max}$, dashed curve for $\epsilon = \epsilon_{min}$. The values of L^* and h_0^* appearing in the figure correspond to $\epsilon = \epsilon_{max}$ (cf. Fig. 3 in Weertman, 1976).

dimensions of velocity. As the model ice sheet has zonal symmetry, we need only look at two-dimensional continuity in a meridional plane. The ablation and accumulation areas A' and A should therefore be taken as lengths rather than areas, where A is the distance between $x = 0$ and $x = L_T$, and A' the distance between $x = L_T$ and $x = L$. By using Eq. (6) for the height profile of the ice and taking into account the isostatic sinking, we obtain

$$\frac{dL^{3/2}}{dt} = \frac{a'}{2\lambda^{1/2}}(\epsilon A - A'), \tag{12}$$

where $\epsilon = a/a'$ is the ratio between the accumulation rate and the ablation rate.

The accumulation rate a is strongly dependent on the snowfall intensity over the accumulation area A. On the time scale of the model, global annual precipitation and evaporation should be nearly equal. Higher globally averaged temperatures T imply that the evaporation is higher and that the oceanic areas where evaporation can take place are also larger. When T is sufficiently low, most of the oceans are covered by ice, and the evaporation is low. Hence, total annual precipitation is an increasing function of temperature. Furthermore, the precipitation rate is assumed to be a weaker function of latitude than of the globally averaged temperature. Thus the quantity a should be an increasing function of temperature. As a first approximation, the ablation a' is taken as constant; hence ϵ is also an increasing function of temperature. Weertman (1976) used a constant value for ϵ, estimated to be about ⅓. In the present model, ϵ is a piecewise linear function of temperature (Fig. 3) given by

$$\epsilon(T) = \begin{cases} \epsilon_{min}, & T \leq T_{\epsilon,lower} \\ \dfrac{\epsilon_{max} - \epsilon_{min}}{T_{\epsilon,upper} - T_{\epsilon,lower}}(T - T_{\epsilon,lower}) + \epsilon_{min}, & T_{\epsilon,lower} < T \leq T_{\epsilon,upper} \\ \epsilon_{max}, & T_{\epsilon,upper} < T. \end{cases} \tag{13}$$

In Eqs. (1b) and (12), $\epsilon(T)$ plays a role similar to the one played in Eqs. (1a), (3) and (5) by $\alpha_{ocean} = \alpha(T)$.

Expressing A and A' in terms of L and L_T, we obtain from (12)

$$\frac{dL}{dt} = \frac{a'}{3(\lambda L)^{1/2}}\{[1 + \epsilon(T)]L_T - L\} \tag{14a}$$

for $L > 0$, and

$$\frac{dL}{dt} = 0 \tag{14b}$$

if $L = 0$. In particular, at equilibrium the ice sheet must satisfy

$$L = [1 + \epsilon(T)]L_T. \tag{15}$$

Using (8) and (15) we can now obtain from (10a) an equation for L as a function of T at equilibrium, i.e., at $dL/dt = 0$,

$$\frac{L}{L^*} = \tfrac{1}{4}\{1 \pm [1 - \beta(T - T_{00})/h_0^*]^{1/2}\}^2, \tag{16a}$$

where

$$L^* = \frac{\epsilon(T)[\epsilon(T) + 1]}{s^2[\epsilon(T) + 2]^2}, \quad h_0^* = \frac{\epsilon(T)}{4s[\epsilon(T) + 2]}. \tag{16b}$$

The equilibrium extent of the ice sheet $L = L(T)$ given by (16) is shown in Fig. 4 for two different fixed values of ϵ. The stability of a given equilibrium ice extent L_0, say, at a fixed temperature T_0, say, is found by considering the linearized form of (14). Stability then corresponds to the derivative of the right-hand side of (14a) with respect to L, evaluated at the point (L_0, T_0), being negative, instability to its being positive. For $T > T_{00} + h_0^*/\beta$, there is only one possible equilibrium state, $L = 0$, and it is linearly stable at fixed T. For $T < T_{00}$, there is also a unique equilibrium width L, which satisfies $L > L^*$, and it is stable with respect to perturbations of L in (14). For a temperature T with $T_{00} < T < T_{00} + h_0^*/\beta$, there are three possible equilibria for the ice width, $0 \leq L$

$< L^*$, the lower and upper ones stable, the middle one unstable.

In our model we shall be mainly interested in states for which T is near T_{00}, and the ice sheet has an extent in the vicinity of its present one. For temperatures close to T_{00} most of the ocean is free from ice and thus ϵ is close to its maximum value. Therefore a suitable scaling for L is L^* obtained from (16b) with $\epsilon(T) = \epsilon_{\max}$, yielding $L^* = 1.3 \times 10^6$ m with our choice of parameter values. The nondimensional variable for the ice width is called l and is defined by

$$l = L/L^*, \tag{17a}$$

with

$$l_T = L_T/L^*. \tag{17b}$$

Introducing this scaling into (10) and (14), we finally obtain

$$c_L \frac{dl}{dt} = l^{-1/2}\{[1 + \epsilon(T)]l_T - l\} \tag{18a}$$

for $l > 0$, with

$$l_T = \frac{1}{L^* s^2}\{[2L^* s^2 l + \beta(T - T_{00})s + \tfrac{1}{4}]^{1/2} - [L^* s^2 l + \beta(T - T_{00})s + \tfrac{1}{2}]\}, \tag{18b}$$

and

$$\frac{dl}{dt} = 0 \tag{18c}$$

for $l = 0$. The time constant c_L is given by

$$c_L = \frac{3}{a'}(\lambda L^*)^{1/2}; \tag{18d}$$

for reasonable values of a', λ and L^* (cf. Weertman, 1976), c_L will be of the order of 10^3 years.

4. Model behavior

By introducing (2), (3) and (18a) into (1), we obtain a system of two coupled equations describing our model. The main physical couplings are in the albedo term and in the temperature dependence of ϵ. Mathematically our system can be described as a system of two nonlinear, ordinary differential equations (ODE's) in the two variables T and l:

$$c_T \frac{dT}{dt} = Q\{1 - [\gamma(\alpha_0 + \alpha_1 L^* l) + (1 - \gamma)\alpha_{\text{ocean}}(T)]\} - k(T - T_0) \equiv P(T,l), \tag{19a}$$

$$c_L \frac{dl}{dt} = l^{-1/2}[(1 + \epsilon(T))l_T(T,l) - l] \equiv R(T,l), \quad l > 0. \tag{19b}$$

The right-hand sides P and R of (19a) and (19b) do not depend on t explicitly; such a system is called *autonomous*.

An important tool for studying the time-dependent behavior of such systems is the phase plane of the variables. Solutions with different initial conditions appear as *trajectories* in the phase plane. For *linear* autonomous systems the behavior of solutions in the phase plane is well known (e.g., Nicolis and Prigogine, 1977, Chaps. 5 and 6).

In *nonlinear* autonomous systems, the location and character of steady states is particularly important in determining the nature of the solutions; the steady states obtain where both $\dot{T} = dT/dt$ and $\dot{l} = dl/dt$ are simultaneously equal to zero. Because of their importance, the points in the T, l phase plane where $P(T,l) = R(T,l) = 0$ are also called *critical points*. The behavior of solutions near the critical point $Q_c \equiv (T_c, l_c)$ can be determined in most cases by linearization around the corresponding steady state, i.e.,

$$T = T_c + x, \quad l = l_c + y.$$

The behavior of the solutions to a linear problem

$$\left.\begin{aligned} \dot{x} &= ax + by \\ \dot{y} &= cx + dy \end{aligned}\right\}, \tag{20a}$$

or, in matrix notation,

$$\dot{\mathbf{z}} = \mathbb{A}\mathbf{z}, \quad \mathbb{A} = \begin{pmatrix} a & b \\ c & d \end{pmatrix}, \quad \mathbf{z} = \begin{pmatrix} x \\ y \end{pmatrix}, \tag{20b}$$

is characterized by the eigenvalues $\lambda = \lambda_r + i\lambda_i$ of the matrix $\mathbb{A} = \mathbb{A}_c$ in (20) (Fig. 5). Clearly, $\mathbb{A}_c$ depends on the critical point around which the linearization was made, $\mathbb{A}_c = \mathbb{A}_c(T_c, l_c)$.

If both eigenvalues of $\mathbb{A}_c$ are real and negative the point $Q_c = (T_c, l_c)$ is a *stable node*. Trajectories in the vicinity of a stable node point toward it and thus solutions starting close to a stable node will eventually reach it. If the eigenvalues are real and positive, Q_c is an *unstable node*. Solutions will move away from the node in this case.

For eigenvalues of $\mathbb{A}_c$ which are real, but of opposite signs, the steady state is called a *saddle point*. Trajectories near a saddle point are similar to hyperbolas; the lines which play the role of asymptotes are called *separatrices*.

Finally, if the eigenvalues have nonzero imaginary parts the steady state is a *focus*. Trajectories will spiral around the steady state in this case, and the stability of these spirals is determined by the signs of the real parts of the eigenvalues. Positive real parts imply an unstable spiral, while stable spirals correspond to $\mathbb{A}_c$ whose eigenvalues have negative real parts. If the real parts are equal to zero, the steady state is a *center* or vortex.

a. The model phase plane

For the system (19a), (19b), we first construct the curves defined by $P(T,l) = 0$ and $R(T,l) = 0$ (Fig.

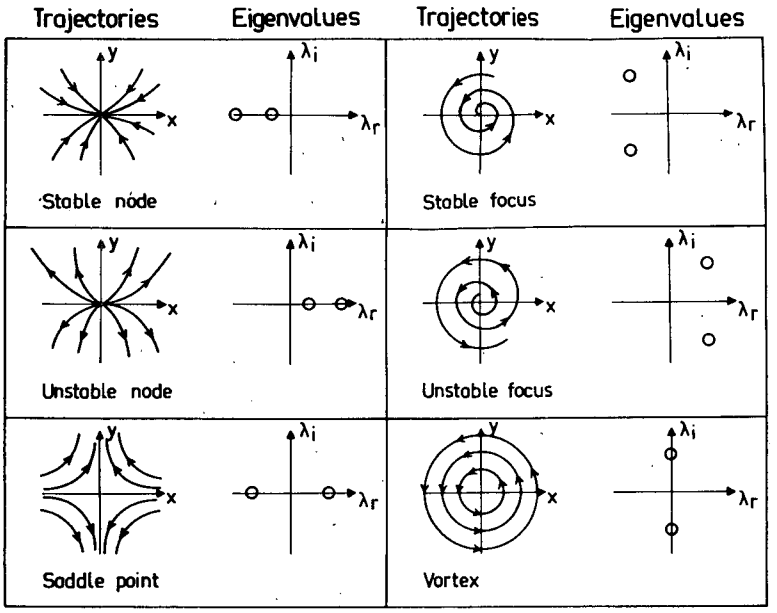

FIG. 5. Classification of phase-plane behavior for a two-dimensional system of linear autonomous ODE's. Solid arrows in x, y diagrams show trajectories, while circles in the λ_r, λ_i diagrams give the corresponding eigenvalues. For further explanation, see text.

6a). The function $P(T,l)$ is linear in l [cf. (19a)] and hence the piecewise linear graph of $P(T,l) = 0$ (dashed curve in Fig. 6a) reflects the linear dependence of R_0 on T [Eq. (2)] and the piecewise linear dependence of α_{ocean} on T (Fig. 3). The function $R(T,l)$ has a somewhat more complicated dependence on l [cf. (19b)] but this dependence departs strongly from linearity only for l small, due to the factor $l^{-1/2}$ in (19b). Thus most of the graph of $R(T,l) = 0$ (dotted curve in Fig. 6a) is still piecewise linear due to the piecewise linear dependence of ϵ on T (Fig. 3); only the last section of this broken line recurves strongly toward the axis $l = 0$ because of the nonlinearity mentioned above. Hence, the detailed shapes of the graphs of $P = 0$ and $R = 0$ are dominated by the temperature dependence of oceanic albedo and of snowfall rates, respectively; in other words, the kinks in the curve $P = 0$ correspond to

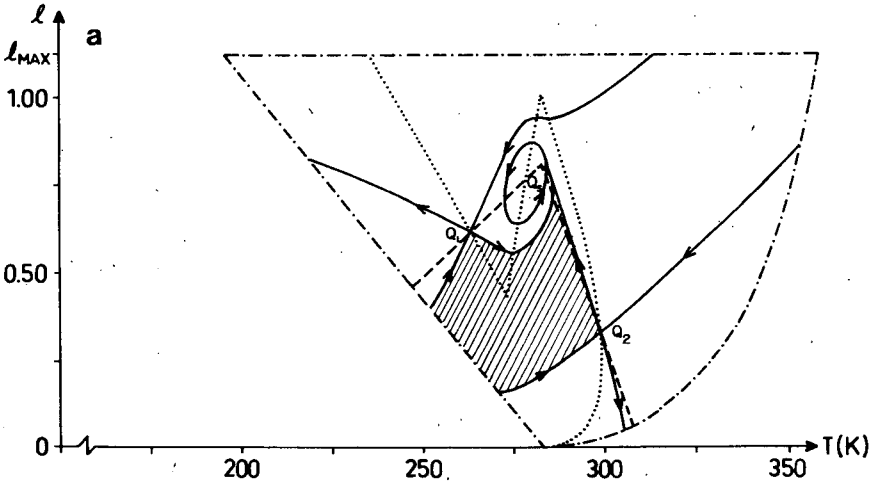

FIG. 6a. The phase plane of the model for a given set of parameter values. Dashed curve shows $P(T,l) = 0$, dotted curve $R(T,l) = 0$. The intersections of these two curves give the steady states of the model. The dashed-dotted curve limits an area inside which the model is physically meaningful. The limit cycle and separatrices (solid curves) show the time-dependent behavior of the model (see text for further explanations).

those in $\alpha_{\text{ocean}}(T)$, while the kinks in $R = 0$ correspond to those in $\epsilon(T)$.

The intersections of these two curves define the steady states of the system. For the parameter values used in Fig. 6, there are four steady states (cf. Källén *et al.*, 1978, Fig. 4a), but we are only interested in those for which our parameterizations are reasonable.

One limit of validity is reached when h_0 is so large that the whole southern half of the land ice sheet is in the ablation zone. The ice sheet will then become stagnant and the land-ice model is no longer valid (Weertman, 1976).

A condition for the non-occurrence of a stagnant ice sheet in terms of T and l can be found by combining (6), (7) and (8), and setting $x = 0$. The condition is

$$T \leqslant (L^*/\beta)[(l/L^*)^{1/2} - sl] + T_{00}. \tag{21}$$

This limit curve given by (21) is the right edge of the dashed-dotted curvilinear triangle in Fig. 6a; it is seen always to be to the right (higher T) of the curve $R = 0$ (dotted).

The opposite limit of validity is reached when the intersection of the 0°C isotherm with the earth's surface is south of the ice sheet. In this case the whole ice sheet is in the accumulation zone, and no steady state can obtain. The condition for this situation not to occur is found by using (7) and (8) with $h = 0$ and $x = L$, giving

$$l \geqslant -\frac{\beta(T - T_{00})}{2sL^*}. \tag{22}$$

The straight line given by (22) is the left edge of the dashed-dotted triangle in Fig. 6a; it is entirely to the left (lower T) of the curve $R = 0$. Furthermore, Eqs. (9a) and (17a) in Section 3 give us a value for $l_{\max}$, which is shown as the horizontal dashed-dotted line in Fig. 6a.

The three conditions above enclose an area in Fig. 6a, inside which our model is physically meaningful; in particular, $l > 0$. In this area there can exist up to five steady states, depending on the choice of parameter values. Fig. 6a shows a situation in which three are present. Denoting points in the (T,l) plane by $Q_j = (T_j,l_j)$, we find by linearizing that the steady states Q_1 and Q_2 are saddle points, while Q_s is a focus. As foci are likely to bifurcate into limit cycles (Andronov *et al.*, 1966, pp. 409–414), we will investigate the properties of Q_s more closely. First, we will look at the local behavior around Q_s, then we will turn to the global picture.

b. Local behavior

From Fig. 6a we see that the focus is located in a temperature range where ϵ increases with T. This increase is actually necessary for the existence of a focus in the model. To find the value of $d\epsilon/dT$ required to produce a focus at Q_s, we consider the condition for the eigenvalues of A_s, the linearization of (P,R) around Q_s, to be complex conjugate. This condition is

$$\frac{d\epsilon}{dT} > \frac{c_L\sqrt{l_s}}{4L^*Q\gamma\alpha_1 l_T(T_s,l_s)} \times \left(\frac{1}{c_L\sqrt{l_s}}\left\{[\epsilon(T_s) + 1]\left(\frac{1}{\sqrt{}} - 1\right) - 1\right\} + k + Q(1 - \gamma)\left(\frac{d\alpha_{\text{ocean}}}{dT}\right)_{T=T_s}\right)^2 - \frac{[\epsilon(T_s) + 1]\beta}{sl_T(T_s,l_s)}\left(\frac{1}{\sqrt{}} - 1\right), \tag{23a}$$

with

$$\sqrt{} = [2sL^*l_s + \beta(T_s - T_{00})s + \tfrac{1}{4}]^{1/2}. \tag{23b}$$

All of the quantities on the right-hand side of (23) are known or have been estimated already, except for α_1.

We showed in Section 3, when motivating the parameterization of ϵ, that $d\epsilon/dT$ should have its maximum value at temperatures below $T_{\alpha,\text{upper}}$, i.e., when sea ice starts to form. For the intersection of $P = 0$ with $R = 0$ corresponding to Q_s to yield a focus, it must occur within the temperature interval in which $d\alpha/dT < 0$ and $d\epsilon/dT > 0$. Assuming $T_{\epsilon,\text{upper}} = T_{\alpha,\text{upper}} = T_{00}$, we can find a condition on the parameters which will guarantee that the maximum value of l attained by the $P = 0$ curve at $T = T_{00}$ will lie below the maximum at the same temperature in the $l = l(T)$ curve defined implicitly by $R(l,T) = 0$. It follows from (19a) with $dT/dt = 0$

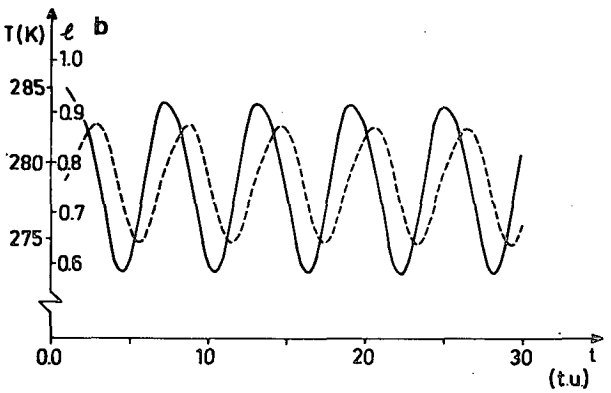

FIG. 6b. Plot of the periodic evolution in time of $T = T(t)$ (solid curve) and $l = l(t)$ (dashed curve) corresponding to the limit cycle in Fig. 6a. One time unit (tu) is the relaxation time (e-folding time) c_T of the atmosphere-ocean-system. Parameter values used are $k = 1.74$ W m^{-2} K^{-1}, $T_0 = 154$ K, $Q = 362.2$ W m^{-2}, $\gamma = 0.3$, $\alpha_0 = 0.25$, $\alpha_1 = 4.1 \times 10^{-7}$ m^{-1}, $\alpha_{\max} = \alpha_{\text{land,max}} = 0.85$, $\alpha_{\min} = 0.25$, $T_{\alpha,\text{upper}} = 283$ K, $T_{\alpha,\text{lower}} = 217$ K, $L^* = 1.3 \times 10^6$ m, $\epsilon_{\min} = 0.1$, $\epsilon_{\max} = 0.5$, $T_{\epsilon,\text{upper}} = 283$ K, $T_{\epsilon,\text{lower}} = 273$ K, $T_{00} = 283$ K, $s = 0.3 \times 10^{-5}$ m$^{-1/2}$, $c_L/c_T = 0.7$.

that this condition can be written as

$$\alpha_1 > \frac{1}{L^*}\left\{\left[1 - (1-\gamma)\alpha_{\text{ocean}}(T_{00}) - \frac{k}{Q}(T_{00} - T_0)\right]\frac{1}{\gamma} - \alpha_0\right\}. \quad (24)$$

This yields a lower bound on α_1 and completes the estimation of quantities appearing in (23).

The stability of the focus can be investigated by inspecting further the eigenvalues of $\mathbf{A}_s$; the sign of their real parts $\lambda_r^{(s)}$ determines the stability of Q_s (see Fig. 5). The transition from a stable focus to an unstable focus often leads to the onset of a limit cycle (Andronov *et al.*, 1966, pp. 635–644) around the focus.

The condition for $\lambda_r^{(s)}$ to be positive, i.e., for Q_s to be unstable, can be written as

$$c_L/c_T > \frac{[\epsilon(T_s)+1]\{[2s^2L^*l_s + \beta(T_s - T_{00})s + \tfrac{1}{4}]^{-1/2} - 1\} - 1}{l_s^{1/2}\left[Q(1-\gamma)\left(\frac{d\alpha_{\text{ocean}}}{dT}\right)_{T=T_s} + k\right]}. \quad (25)$$

When c_L/c_T exceeds the critical value given by (25), the stable focus will turn into a locally unstable focus. Notice here that the values of c_L and c_T do not affect the position of the curves $P = 0$ and $R = 0$.

The stability properties of the focus Q_s can thus change without its position changing. Physically, condition (25) states that the development of the land ice sheet has to be slow enough compared to the thermal relaxation time of the ocean in order for self-excited oscillations to obtain.

c. Global behavior

The saddle points Q_1 and Q_2 have ingoing and outgoing separatrices as shown in Fig. 6a. Each ingoing separatrix of a saddle point acts as a "ridge", dividing the flow of trajectories in the phase plane into separate regions. Within the area of the dashed-dotted triangle in Fig. 6a, there are two such "ridges" formed by the ingoing separatrices of Q_1 and Q_2, respectively. These divide the area into three separate regions. A trajectory in one of the regions cannot cross a "ridge" into another region, but has to stay within the region it started in.

The middle region contains the focus Q_s; the two separatrices going out from Q_1 and Q_2, respectively, into the middle region are seen to spiral in toward the focus. When the focus is unstable, however, the separatrices cannot reach Q_s; this makes the existence of a limit-cycle around Q_s very plausible.

By numerical experimentation a limit cycle has indeed been found around Q_s for a whole range of parameter values. This limit cycle is shown in Fig. 6a and the corresponding plot of temperature T and land-ice extent l versus time is shown in Fig. 6b; the set of parameter values used for the computation illustrated is given in the figure caption. One time unit (tu) in Fig. 6b is equal to the relaxation time c_T of the energy-balance equation for the ocean-atmosphere system. This time unit can be interpreted as the overturning time for the oceans, and an estimate commonly used is of the order of 10^3 years.

The region of the T, l phase plane bounded by the two outgoing separatrices converging on the limit cycle, by the two adjacent ingoing separatrices from the left (lower T), and by the portion of the dashed-dotted validity boundary between the latter is called an elementary *cell* (Andronov *et al.*, 1966, pp. 374–404); this cell is hatched in Fig. 6a. The qualitative theory of autonomous systems allows us to infer that the flow in this cell tends toward a *stable* limit cycle. Furthermore the cell itself is stable under perturbations of the system (19), i.e., this type of cell is a feature of a *structurally stable* system (Andronov *et al.*, 1966, Figs. 309–310, Cases BIIb_2 and $\bar{\text{B}}\text{IIb}_2$).

Numerical computations confirmed that all trajectories in the previously mentioned middle region converged to the limit cycle, i.e., that the limit cycle is asymptotically stable for the parameter values used in Fig. 6. Further numerical experimentation showed that the same asymptotic stability obtains for a wide range of parameter values around the one illustrated, i.e., the limit cycle is also *structurally* stable.

The most interesting parameter, as seen from condition (25), is the ratio c_L/c_T. We have determined numerically the dependence on c_L/c_T of the limit cycle's amplitude $(\Delta T, \Delta l)$, oscillation period τ and phase lag ϕ of ice extent l behind temperature T. Fig. 7 shows this dependence for a range of c_L/c_T values above the critical one determined from (25).

When c_L/c_T reaches its critical value, the amplitude of the onsetting limit cycle jumps from zero directly to the value indicated in Fig. 7. A possible explanation of this jump could be subcritical bifurcation (Andronov *et al.*, 1966, Fig. 495; Marsden and McCracken, 1976, p. 8), in which an unstable limit cycle exists between the focus and the stable limit cycle for a certain range of values of c_L/c_T below the critical one. Other possibilities, such as the exist-

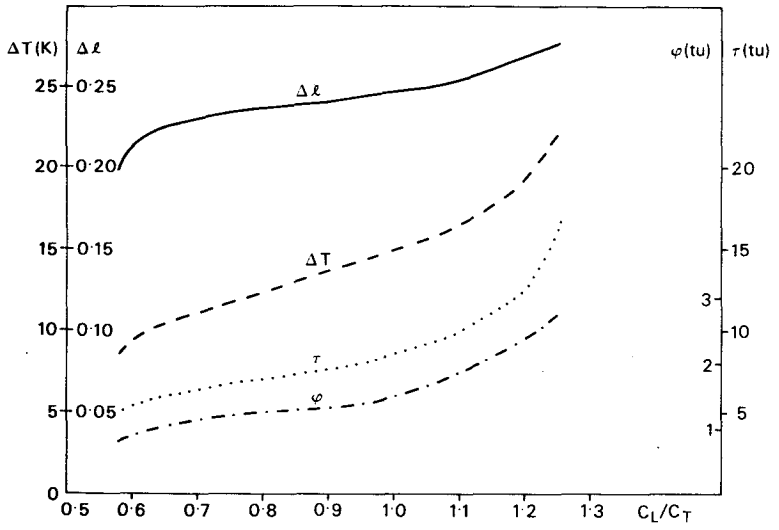

FIG. 7. Plot of the limit-cycle amplitude in T (ΔT) and in l (Δl) and of the limit-cycle period (τ) and phase lag (ϕ) as functions of c_L/c_T. One time unit (tu) is the relaxation time c_T of the atmosphere-ocean system.

ence of a branch of quasi-periodic solutions connecting the end points of the jump, would also have to be considered. We have not performed the delicate numerical computations which would be required to study model behavior in this region, since it appeared to be less interesting physically.

For values of c_L/c_T above the critical one, both the amplitudes and the period of the limit cycle increase smoothly until an upper critical value in c_L/c_T is reached. At this point the limit cycle becomes so large that it touches the saddle point Q_1 and the limit cycle merges with the upper ingoing separatrix to Q_1. For larger values of c_L/c_T there exists no limit cycle around Q_s within the region of validity of the model.

5. Discussion and conclusions

The model presented here exhibits limit-cycle behavior for a certain range of parameter values and of initial conditions. The amplitude, phase lag and oscillation period of the stable periodic solutions obtained are of the same order of magnitude as those associated with glaciation cycles. To the extent that one can show the range of parameter values used in the model to be reasonably realistic, the results suggest that this model describes an internal physical mechanism capable of producing glaciation cycles in the absence of periodic exterior forcing.

This physical mechanism can be described as follows: If one starts out with a situation in which temperatures are so high that there is very little sea ice or none (cf. Fig. 6b, near $t = 0$), then the evaporation and consequently the snowfall rates are also high. This will start a buildup of the glaciers, which in turn will increase the albedo. When albedo increases, temperature will decrease and thus snowfall rates will decrease. The glacier buildup slows down because of the snowfall decrease and eventually stops. The situation now is one of maximum glacial extent and of decreasing temperatures. A further decrease in temperature will cause the glaciers to retreat because of the still decreasing snowfall rate. Eventually, the glacier retreat will cause a decreased albedo and the temperature will go up. Because of the inertia of the glaciers' plastic flow, this temperature rise will not immediately produce rapidly growing glaciers, the temperature will reach its maximum value before the glacier has had time to build up, and the system is back to the situation described in the beginning. However, if the glacier flow is too slow, it will not have had the time to reach its maximum extent while the temperature is still decreasing, and thus the temperature will continue to decrease. This is the case when c_L/c_T has reached its upper critical value and the limit cycle vanishes. When c_L/c_T is below its lower critical value, on the other hand, glacier and temperature variations cannot be sufficiently out of phase for oscillations to occur.

A characteristic feature of the limit cycle is the phase difference ϕ between the glacial extent l and the temperature T (Fig. 7). Broecker (1978) has observed such a phase lag in his comparative study of paleoclimatic data; this observation suggests very strongly that internal mechanisms are involved in climatic variations on time scales of the order of 10^3–10^5 years. It is noteworthy that our results show temperature leading glacial volume in phase, in accordance with recent paleoclimatological evi-

dence. This evidence shows the coexistence of low sea-surface temperatures (SST's) with low continental ice volumes (Hays and Cooke, 1978), and of high SST's with large continental ice sheets (Ruddiman and McIntyre, 1979).

Sergin (1979)[2], has studied a somewhat more complicated model than ours, in which energy balance, glacial dynamics and lithosphere dynamics are considered separately for the two hemispheres. Self-sustained oscillations also obtain in his model when glaciers are present, as was the case in our simple model.

The presence and slow evolution of the continental ice sheets are clearly essential for the existence of periodic solutions to the model equations. One may speculate that this could explain the absence of large, periodic temperature oscillations during the extended warm periods of the earth's past, in which such ice sheets were absent.

The mechanisms by which continental ice sheets first appear occur on a longer time scale than the one considered here (Emiliani and Geiss, 1957). The model seems to show that once they are established and reach a certain extent, their size will oscillate, as will the global temperature. The range of the oscillations for realistic parameter values seems to give ice margins never reaching back to the Arctic Ocean, nor forward to the equator.

An essential parameter in our model is ϵ, the precipitation efficiency; for oscillatory behavior to occur, it is necessary to have an increase of ϵ with temperature. This increase in $\epsilon(T)$ plays here a role analogous to the role of the decrease in $\alpha(T)$ for the stationary, non-oscillatory energy-balance models and the multiplicity of their equilibria (Budyko, 1969; Sellers, 1969; Ghil, 1976; Crafoord and Källén, 1978). The increase in ϵ with T has been shown to be the result of a plausible physical mechanism, namely the one which on much shorter time scales causes larger snowfall in warmer winters. The magnitude of this increase which is necessary in order to produce oscillations can be calculated as a function of all the other parameters [cf. Eq. (23)]. It is difficult at present to compare our estimates of $d\epsilon/dT$ quantitatively with observations; reliable numerical estimates for such global quantities, based on contemporary observations, are hard to obtain.

The present model is only a first attempt to investigate whether a coupled atmosphere-hydrosphere-cryosphere system can give rise to self-sustained oscillations. In order to be able to represent physical phenomena more realistically, we are presently studying a latitudinally dependent model. The physical mechanism behind the glacial dynamics is the same, but the latitudinal dependence makes it possible to have more realistic parameterizations of local snowline height, snowfall rates, albedo values, etc. (Crafoord, 1979).[3]

A latitudinally dependent model can also be compared more directly with the one studied by Bhattacharya and Ghil (1978). In their model, a prescribed time lag is introduced into the temperature dependence of the albedo. This time lag represents implicitly the ice-sheet dynamics in their latitude-dependent model and also gives rise to the existence of periodic solutions (Ghil and Bhattacharya, 1979).

For certain parameterizations, their model exhibits bounded nonperiodic solutions (Lorenz, 1963); such behavior is not possible in a model involving only two coupled ODE's. The latitudinal dependence will introduce more degrees of freedom, and that may lead to nonperiodic behavior in our modified model.

It would also be interesting as a next step to study the combined effect of internal and external agencies on a model system such as the one presented here, in other words, to study *forced* oscillations of a nonlinear climatic oscillator. The model's nonlinearities may possibly give rise to subharmonics, i.e., to solutions whose period is a multiple of the period in the forcing. Such subharmonic model response could account for the 100 000 year cycle observed in the paleoclimatic records, but not found with a sufficient amplitude in the astronomical forcing (Berger, 1977).

Acknowledgments. It is a pleasure to acknowledge constructive discussions with Bert Bolin and Henning Rodhe. Suggestions by Wallace S. Broecker and Gerald R. North were also very useful. The final manuscript benefited from a careful reading by Eugene Isaacson, Hilding Sundqvist and Katia Laval and from the reviewers' comments.

Part of this work was carried out while one of the authors (M.G.) was a Visiting Professor at the International Meteorological Institute in Stockholm. His work at the Courant Institute was supported by NASA Grant NSG-5130.

REFERENCES

Andronov, A. A., A. A. Vitt and S. E. Khaikin, 1966: *Theory of Oscillators*. Pergamon Press, 815 pp.

Berger, A. L., 1977: Support for the astronomical theory of climatic change. *Nature*, **269**, 44–45.

Bhattacharya, K., and M. Ghil, 1978: An energy-balance model with multiply-periodic and quasi-chaotic free oscillations. *Evolution of Planetary Atmospheres and Climatology of the Earth*, Centre National d'Études Spatiales, 299–310.

[2] *Note added in proof*: The authors became aware of the work of V. Ya. Sergin, S. Ya. Sergin and their associates on the GOA model (private communications of G. R. North and of T. M. L. Wigley, 1978) only after the research reported herein was essentially complete. Results on the GOA model became available in English as Sergin (1979) while this article was in print.

[3] Ph.D. thesis, in preparation.

Broecker, W. S., 1978: The cause of glacial to interglacial climatic change. *Evolution of Planetary Atmospheres and Climatology of the Earth,* Centre National d'Études Spatiales, 165–190.

Budyko, M. I., 1969: The effect of solar radiation variations on the climate of the earth. *Tellus,* **21,** 611–619.

Crafoord, C., and E. Källén, 1978: A note on the condition for existence of more than one steady-state solution in Budyko-Sellers type models. *J. Atmos. Sci.,* **35,** 1123–1125.

Emiliani, C., and J. Geiss, 1957: On glaciations and their causes. *Geol. Rundsch.,* **46,** 576–601.

Ghil, M., 1976: Climate stability for a Sellers-type model. *J. Atmos. Sci.,* **33,** 3–20.

——, and K. Bhattacharya, 1979: An energy-balance model of glaciation cycles. *A Review of Climate Models: Performance, Intercomparison and Sensitivity Studies,* W. L. Gates, Ed., GARP Publ., Ser., WMO, 886–916.

Hays, J. D., and D. W. Cooke, 1978: Factors contributing to glacial-interglacial climate changes. *Evolution of Planetary Atmospheres and Climatology of the Earth,* Centre National d'Études Spatiales, p. 157.

——, J. Imbrie and N. J. Shackleton, 1976: Variations in the earth's orbit: Pacemaker of the ice ages. *Science,* **194,** 1121–1132.

Källén, E., C. Crafoord and M. Ghil, 1978: Free oscillations in a coupled atmosphere-hydrosphere-cryosphere system. *Evolution of Planetary Atmospheres and Climatology of the Earth,* Centre National d'Études Spatiales, 285–297.

Kominz, M. A., and N. G. Pisias, 1979: Pleistocene climate: Deterministic or stochastic?, *Science,* **204,** 171–173.

Lorenz, E. N., 1963: Deterministic nonperiodic flow. *J. Atmos. Sci.,* **20,** 130–141.

Marsden, J. E., and M. McCracken, 1976: *The Hopf Bifurcation and its Applications.* Springer, 408 pp.

Mitchell, J. M., Jr., 1976: An overview of climatic variability and its causal mechanisms. *Quat. Res.,* **6,** 481–493.

Nicolis, G., and I. Prigogine, 1977: *Self-Organization in Non-Equilibrium Systems.* Wiley-Interscience, 491 pp.

Ruddiman, W. F., and A. McIntyre, 1979: Warmth of the subpolar North Atlantic Ocean during Northern Hemisphere ice-sheet growth. *Science,* **204,** 173–175.

Sellers, W. D., 1969: A global climatic model based on the energy balance of the earth-atmosphere system. *J. Appl. Meteor.,* **8,** 392–400.

Sergin, V. Ya., 1979: Numerical modeling of the glacier-ocean-atmosphere global system. *J. Geophys. Res.,* **84,** 3191–3204.

Weertman, J., 1964: Rate of growth or shrinkage of non-equilibrium ice-sheets. *J. Glaciol.,* **6,** 145–158.

——, 1976: Milankovich solar radiation variations and ice-age ice-sheet sizes. *Nature,* **261,** 17–20.